8C.1 THE SYNERGISTIC EFFECT OF MID-LEVEL DRY AIR AND VERTICAL WIND SHEAR ON TROPICAL CYCLONE VENTILATION PATHWAYS

Joshua J. Alland*, Brian H. Tang, and Kristen L. Corbosiero
University at Albany, State University of New York, Albany, New York

1. INTRODUCTION

Dry air and vertical wind shear (VWS) can work together to affect tropical cyclone (TC) development via ventilation. Ventilation occurs when TC structural changes, due to VWS, act to flux low-moist static energy (MSE) air from the environment into the high-MSE reservoir of the inner core (Simpson and Riehl 1958; Cram et al. 2007; Marín et al. 2009; Riemer et al. 2010; Tang and Emanuel 2012a,b; Munsell et al. 2013), frustrating the TC heat engine.

Previous studies have documented different ventilation pathways and their effects on mature TCs. Dry air can ventilate midlevels (mid-level pathway) and reduce the MSE of rising parcels in the eyewall. Dry air can also ventilate the subcloud layer (low-level pathway), via either convective downdrafts (Riemer et al. 2010) or subsidence associated with the downward branch of the TC secondary circulation (Alland et al. 2017).

The relative importance of the mid- and low-level ventilation pathways, and the situations in which these pathways operate, remain unclear (Riemer and Laliberté 2015). Previous literature has studied ventilation pathways in mature TCs from an axisymmetric perspective (Tang and Emanuel 2012a), but the structure of these ventilation pathways during early development in a 3D model is unexplored. Previous literature has also relied on case studies (Cram et al. 2007) or modeling studies with differing magnitudes of VWS (Riemer et al. 2010; Riemer and Montgomery 2011), but the structure of these ventilation pathways may depend on the magnitude of the VWS *and* the thermodynamic environment, such as the mid-level moisture content.

This study will investigate the structure of ventilation pathways in a moisture–VWS bivariate parameter space to gain a better understanding of these structures during early development, which is vital to improving forecasts of TC intensity change.

2. MODELING FRAMEWORK

This study employs a set of 3D idealized simulations using Cloud Model 1 (CM1) (Bryan and Fritsch 2002). Each simulation has a constant initial relative humidity (RH) above the subcloud layer, ranging from 20 to 80%, and a specified westerly VWS magnitude, ranging from 0 to 12.5 m s^{-1}, as shown in Fig. 1.

* *Corresponding author address:* Joshua J. Alland, University at Albany, State University of New York, 1400 Washington Avenue, DAES 325, Albany, NY 12222; email: jalland@albany.edu.

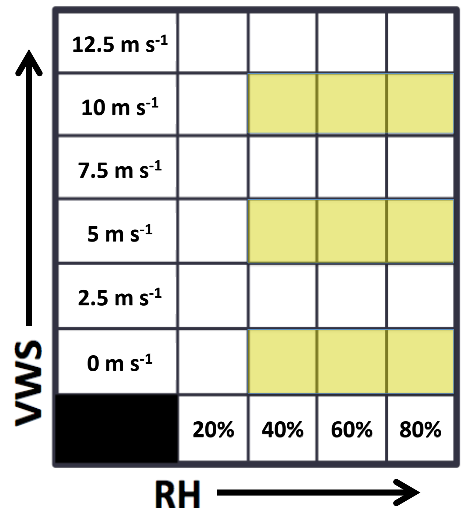

Figure 1: *The RH–VWS bivariate parameter space. Each grid box represents one simulation. Only the simulations highlighted in yellow are analyzed below.*

Figure 2 shows the evolution of the maximum, azimuthally-averaged 10-m wind for the simulations highlighted in yellow in Fig. 1. When no VWS exists (solid lines), intensification occurs sooner for a moister initial environment, in agreement with Tang et al. (2016). For a VWS of 5 m s^{-1} (thin, dashed lines), intensification starts earlier than when no VWS exists, especially for moister simulations, but the intensification rate is not as large thereafter. For a VWS of 10 m s^{-1} (bold, dashed lines), intensification occurs more slowly. In fact, the simulation with an initial RH of 40% does not reach 20 m s^{-1}.

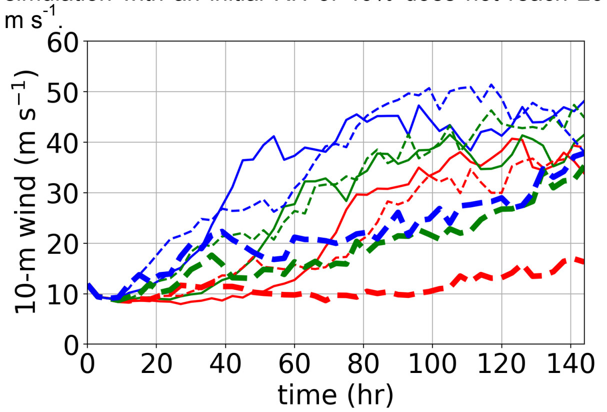

Figure 2: *Time series of the maximum, azimuthally-averaged 10-m wind speed with an initial RH of (red) 40%, (green) 60%, and (blue) 80%, and an initial VWS magnitude of (solid) 0 m s^{-1}, (thin dashed) 5 m s^{-1}, and (bold dashed) 10 m s^{-1}.*

3. MID-LEVEL VENTILATION

Mid-level ventilation is given by $\rho u's'$, where u is the storm-relative radial velocity, s is the MSE, and primes denote perturbations from the azimuthal mean. This term represents the lateral transport of MSE by eddies (Tang and Emanuel 2010), and will be compared across the bivariate parameter space to determine the structure of mid-level ventilation.

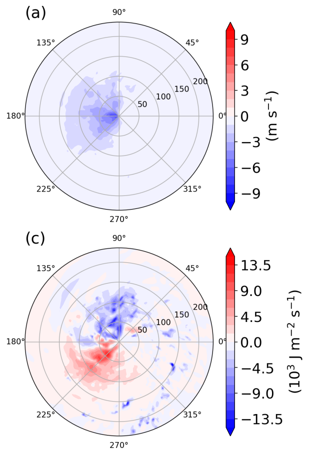

Figure 3: *Spatial distribution of (a) u', (b) s', and (c) ρu's' at 700 hPa, averaged over the early development period, for an initial RH of 40% and VWS magnitude of 5 m s^{-1}. Only values where u'<0 are plotted. The center of the plot represents the center of the TC at 850 hPa.*

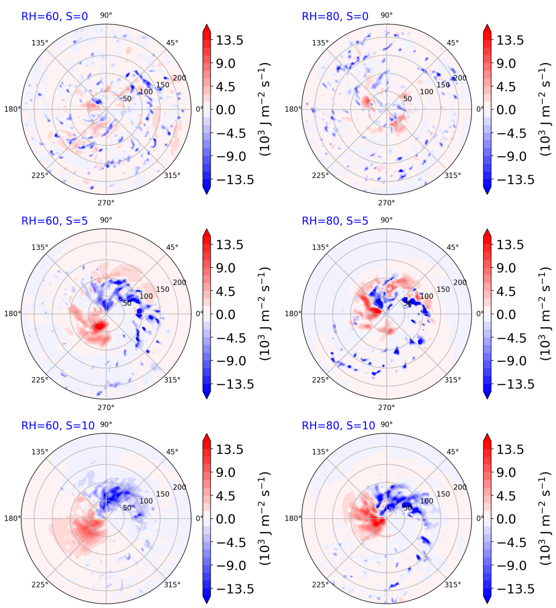

Figure 4: *Spatial distribution of ρu's' at 700 hPa, averaged over the early development period, for simulations in the bivariate parameter space. Only values where u'<0 are plotted. The initial RH and VWS magnitude is given at the upper-left of each figure.*

Figure 3a shows *u'* at 700 hPa for the simulation with an initial RH of 40% and a VWS of 5 m s^{-1}, averaged over the early development period. This period is defined between model initialization and the time that minimal hurricane intensity (20 m s^{-1}) is reached. Note that we only concentrate on areas where *u'*<0 to isolate the inward flux of low-MSE midlevel air. Storm-relative inflow occurs upshear within the inner-150 km, representing westerly, storm-relative flow (in the direction of the VWS vector). Figure 3b shows *s'*, which is generally positive to the left, and negative to the right, of the VWS vector within the inner-150 km.

Figure 3c shows that positive values of ρ *u's'* occur in the upshear-right quadrant within the inner-150 km, representing the storm-relative, inward transport of low-MSE air into the high-MSE TC core. Thus, mid-level ventilation preferentially occurs in the upshear-right quadrant during early development in this simulation.

Figure 4 shows ρ *u's'* for a subset of simulations in the bivariate parameter space with initial RH values of 60 and 80%, and VWSs of 0, 5, and 10 m s^{-1}. For no VWS, ρ *u's'* has no clear pattern. As the VWS increases, a more coherent pattern emerges with positive values in the upshear semicircle. This pattern encompasses a larger area as the VWS magnitude increases, and moves into the upshear-right quadrant as the initial RH decreases. Other vertical levels above 700 hPa show a similar pattern.

4. LOW-LEVEL VENTILATION

Low-level ventilation is given by ρ *w's'*, where *w* is the vertical velocity. This term represents the vertical transport of MSE by shear-induced downdrafts (Riemer et al. 2010), and is compared across the bivariate parameter space to determine the structure of low-level ventilation (Fig. 5). Note that we only concentrate on areas where *w'*<0 to isolate the downward flux of low-MSE at 850 hPa. For no VWS, generally positive values of ρ *w' s'* exist and are distributed symmetrically about the center. With the addition of VWS, positive values of ρ *w' s'* exist to the right of the VWS vector inside a radius of 50 km and to the left of the shear vector outside a radius of 50 km. The positive values represent the flux of low-MSE air into the subcloud layer.

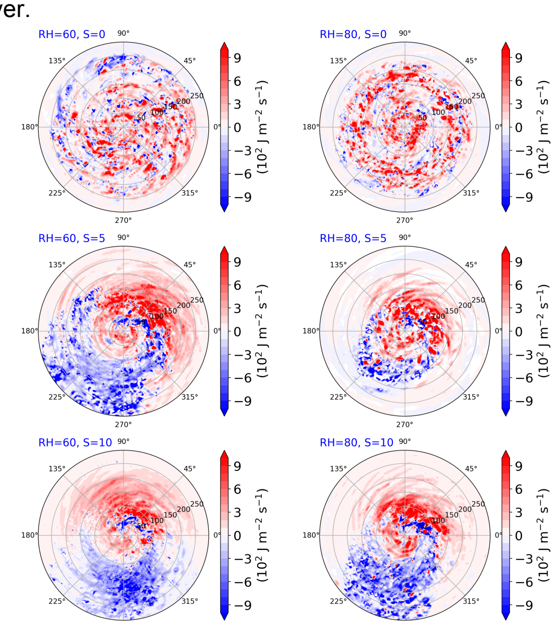

Figure 5: *Same as Fig. 4, but for ρw's' at 850 hPa. Only values where w'<0 are plotted.*

This study explored how the spatial structure of mid- and low-level ventilation varies as a function of both RH and VWS during early development. These ventilation pathways can decrease the strength of convection and inhibit TC development, so understanding the structure of ventilation provides new insight into their effects on the structure of convection and controls on TC intensity, which is the subject of complementary and future work.

References

Alland, J. J., B. H. Tang, and K. L. Corbosiero, 2017: Effects of midlevel dry air on development of the axisymmetric tropical cyclone secondary circulation. *J. Atmos. Sci.*, **74**, 1455–1470.

Bryan, G. H., and J. M. Fritsch, 2002: A benchmark simulation for moist nonhydrostatic numerical models. *Mon. Wea. Rev.*, **130**, 2917–2928.

Cram, T. A., M. T. Montgomery, and S. A. Braun, 2007: A Lagrangian trajectory view on transport and mixing processes between the eye, eyewall, and environment using a high-resolution simulation of Hurricane Bonnie (1998). *J. Atmos. Sci.*, **64**, 1835–1856.

Marín, J. C., D. J. Raymond, and G. B. Raga, 2009: Intensification of tropical cyclones in the GFS model. *Atmos. Chem. Phys.*, **9**, 1407–1417.

Munsell, E. B., F. Zhang, and D. P. Stern, 2013: Predictability and dynamics of a nonintensifying tropical storm: Erica (2009). *J. Atmos. Sci.*, **70**, 2505–2524.

Riemer, M., and F. Laliberté, 2015: Secondary circulation of tropical cyclones in vertical wind shear: Lagrangian diagnostic and pathways of environmental interaction. *J. Atmos. Sci.*, **72**, 3517–3536.

Riemer, M., and M. T. Montgomery, 2011: Simple kinematic models for the environmental interaction of tropical cyclones in vertical wind shear. *Atmos. Chem. Phys.*, **11**, 9395–9414.

Riemer, M., and M. T. Montgomery, and M. E. Nicholls, 2010: A new paradigm for intensity modification of tropical cyclones: Thermodynamic impact of vertical wind shear on the inflow layer. *Atmos. Chem. Phys.*, **10**, 3163–3188.

Simpson, R., and R. Riehl, 1958: Mid-tropospheric ventilation as a constraint on hurricane development and maintenance. *Tech. Conf. on Hurricanes*, Amer. Meteor. Soc., Miami Beach, FL, D4–1-D4–10.

Tang, B., and K. Emanuel, 2010: Midlevel ventilation's constraint on tropical cyclone intensity. *J. Atmos. Sci.*, **67**, 1817–1830.

Tang, B., and K. Emanuel, 2012a: Sensitivity of tropical cyclone intensity to ventilation in an axisymmetric model. *J. Atmos. Sci.*, **69**, 2394–2413.

Tang, B., and K. Emanuel, 2012b: A ventilation index for tropical cyclones. *Bull. Amer. Meteor. Soc.*, **93**, 1901–1912.

Tang, B. H., R. Rios-Berrios, J. J. Alland, J. D. Berman, and K. L. Corbosiero, 2016: Sensitivity of axisymmetric tropical cyclone spinup time to dry air aloft. *J. Atmos. Sci.*, **73**, 4269–4287.